Transient receptor potential protein (Trp) mRNA expression in rat substantia nigra

Transient receptor potential protein (Trp) mRNA expression in rat substantia nigra

by

Jordan B. Sylvester

A Thesis Submitted to the School of Graduate Studies

in Partial Fulfillment of the Requirements For the Degree

Master of Science

McMaster Univesity

September, 2000

Master of Science (2000) McMaster University

(Biology) Hamilton, Ontario

Title: Transient receptor potential protein (Trp) mRNA expression in rat substantia nigra.

Author: Jordan B. Sylvester, H.B.Sc. (University of Guelph)

Supervisor: Dr. Ashok K. Grover

Number of Pages: x, 55

This thesis is dedicated to my grandfather, William G. Howson.

Abstract

Substantia nigra neurons produce dopamine in response to cholinergic stimuli that may involve receptor operated Ca^{2+}-entry that has been associated with the transient receptor potential (Trp) proteins. There were 6 Trp isoforms reported when I started this work. I set out to determine which isoforms of Trp mRNA were expressed in the substantia nigra using the whole brain for comparison. I initially used RT-PCR to determine the Trp mRNA expression. Subsequently, I used competitive RT-PCR for quantifying the major isoforms. Finally, I confirmed my results by Co-RT-PCR of the major isoforms. Trp3 and Trp6 were found to be the predominant forms expressed in the substantia nigra and whole brain, while the levels of Trps 1, 2, 4 and 5 were very low in both. Estimation of mRNA levels using competitive RT-PCR showed that the Trp6 mRNA levels in substantia nigra and the whole brain were similar while those for Trp3 were significantly lower in the substantia nigra than in the whole brain. Thus substantia nigra differs from the whole brain in its Trp expression. Properties of Trps 3 and 6 are not fully known. Trp3 is regulated by IP_3-receptor activation but both Trp 3 and 6 can be activated by diacylglycerol. How this relates to the signal transduction events in substantia nigra remains to be determined.

Acknowledgements

I would like to express a special thanks to my supervisor, Dr. Ashok K. Grover, for his patience, guidance and support during the past two years. He has helped to develop both my scientific understanding and my character.

To all of my colleagues in 4N75, I thank you for your guidance and friendship. Special thanks to Dr. Susan Lacosta, Cia Barlas, Kirsten Culver and Dr. R. Mishra for their direction regarding rat brain dissection, and to Melanie Holmes, James Mwanjewe and Catherine Sylvester for reviewing this report, and to Dr. D. Harnish for being a member of my supervisory committee.

Thanks to Douglas Mack for taking a keen interest in both my work and my life. His friendship during these past two years will always be remembered.

I would also like to thank Dr. Mike Zhu, Ohio State University, for sharing his knowledge of Trp proteins.

I am grateful for the love and support of my family through what has been a most challenging time of my life.

Finally, I would like to thank God for maintaining a strong grip on my heart through life's ups and downs. Amen.

This work was supported in part by the Medical Research Council of Canada.

Table of Contents

List of Figures

List of Tables

Abbreviations

Trp =	Transient Receptor Potential
PCR =	Polymerase Chain Reaction
RT-PCR =	Reverse Transcriptase – PCR
DNase =	Deoxyribonuclease
G3PDH =	Glyceraldehyde-3-Phosphate Dehydrogenase
IP_3 =	Inositol 1, 4, 5 -triphosphate
IP_3R =	IP_3 Receptor
PIP_2 =	Phosphatidylinositol 4, 5-biphosphate
VOC =	Voltage-Operated Calcium Channel
ROC =	Receptor-Operated Calcium Channel
PLC =	Phospholipase C
DAG =	Diacylglycerol
INAD =	Inactivation No-Afterpotential D
PDZ =	A domain named after three of the proteins in which the repeats have been described: PSD-95 (postsynaptic density protein, M_r 95K), Dlg (*discs-large* protein) and ZO-1 (zonula occludens-1).
SN =	Substantia nigra
SNpc =	SN pars compacta
MOPS =	3-[N-Morpholino] propanesulfonic acid
DEPC =	Diethyl Pyrocarbonate
DTT =	Dithiothreitol

EDTA = Ethylene-diaminetetra acetic acid

dNTP = Deoxyribonucleotide 5'-triphosphate

SERCA = Sarco/Endoplasmic Reticulum Calcium ATPase

1. Introduction

The objective of these experiments was to determine the distribution of transient receptor potential (Trp) mRNAs in the substantia nigra and in the whole brain of rat. To fully develop the rationale for this research I will briefly describe cell calcium regulation, store-operated calcium entry, and the discovery, characterization and regulation of the Trp genes in *Drosophila* and mammalian cells.

1.1 Regulation of Cellular Calcium

Calcium influx plays a fundamental role in the regulation of many cell signaling events, including those involved in growth, differentiation and physiology. Although cytosolic calcium concentration is normally low, it can be immediately elevated, in response to stimulation, via calcium-permeable channels in the plasma membrane or on the internal calcium stores (or calciosomes). Extracellular calcium entry is traditionally thought to be mediated by either voltage-operated or receptor-operated calcium channels (VOC & ROC, respectively). Release of calcium from the calciosomes is activated in a receptor-operated manner using the phosphoinositide (PI) signaling system (3). Here, the stimulation of a G-protein coupled receptor causes its associated heteromeric G-protein to activate phospholipase C (PLC) (3). Once activated, PLC catalyzes the

hydrolysis of membrane-associated phosphatidylinositol-4,5-bisphosphate (PIP_2) to inositol triphosphate (IP_3) and diacylglycerol (DAG) (3). IP_3, then, relays the message to the calciosomes by stimulating IP_3-transmembrane receptors (Type 3 IP_3Rs) to open and liberate Ca^{2+} (3). In order to return the concentration of cytoplasmic calcium to baseline, cells export Ca^{2+} out of the cytoplasm through the plasma membrane via sodium/calcium exchange and plasma membrane calcium-ATPase, and back into the calciosomes through sarco-/endoplasmic reticulum calcium ATPases (2). Such tight regulation of calcium entry and exit creates a complex spatial and temporal gradient, which allows calcium to be involved in a diverse array of cellular functions.

1.2 Store-Operated Calcium Entry

Unlike the extracellular mileau, the calciosomes contain a finite amount of calcium and must be refilled. Many publications have described a measurable inward-rectifying current in non-excitable cells whose calciosomes have been depleted (46, 52, 53). This current has been characterized and designated Ca^{2+} release-activated Ca^{2+} current (I_{CRAC}) and the channels responsible are known as store-operated calcium (SOC) channels.

The mechanism by which store depletion initiates SOC channel opening remains unresolved, yet, three main theories have been proposed: 1) a diffusable messenger, 2) conformational coupling, and 3) channel insertion (72). The first proposes that a diffusable molecule is released or is activated by Ca^{2+}- release

from the calciosomes and travels to its SOC channel target on the plasma membrane (72). The conformational coupling model suggests that IP_3R modulates SOC channel opening through direct protein-protein interaction with it (24A). The third theory submits that SOC channels are inserted into the plasma membrane via the endocytosis of intracellular vesicles, in response to calciosome depletion (24A).

1.3 Transient Receptor Potential Protien Channels

1.3.1 *Drosophila* Photoreceptor

Although I_{CRAC} can be observed in most mammalian cells, the proteins which make-up SOC channels are still under investigation. The most likely candidate is a mammalian homolog for the *Drosophila* protein named Trp (11, 35, 47). *Drosophila* photoreceptors are unique in that they lack both voltage-operated and (traditional) receptor-operated calcium channels. Therefore, calcium influx must be mediated by an alternative channel. The photoreceptors of mutant flies which lack Trp display a calcium influx current which produces a transient receptor potential (Trp) in response to light (11, 35, 47). These flies display normal phototaxis but behave as though blind during prolonged exposure to light. Although wildtype photoreceptors produce the same transient upstroke of receptor potential it is always followed by a weaker, sustained phase (11, 35, 47). Moreover, the Ca^{2+} selectivity of *Trp*$^{-}$ mutant channels is reduced by ~10-fold.

Therefore, it is this sustained, Ca^{2+}-selective influx current which is important to sight, and which appears to be modulated by Trp (11, 35, 47).

1.3.1a Protein Characterization

The proposal that Trp encodes an ion channel was developed through the molecular identification of the gene (11, 35, 47). Kyte-Doolittle hydrophobicity plots of the 1275-amino acid Trp protein indicate that it contains multiple transmembrane domains; the predicted structure bears striking sequence similarity to both voltage- and second messenger-gated ions channels. However, if Trps form an ion channel, it is not voltage operated because Trp proteins lack the positively charged arginine residues found in the fourth transmembrane region of VOC channel proteins which are thought to act as a voltage sensor (11, 35, 47). Moreover, both single channel and whole cell recordings have verified that Trp proteins form voltage-independent, Ca^{2+}-selective channels which respond to calciosome depletion, *in vitro*.

During a screen for calmodulin binding proteins in the *Drosophila* head, an 1124-residue protein was discovered, named Trp-like (or Trpl); due to a 40% sequence identity with Trp over approximately 700 amino terminal residues (18, 29). Like Trps, Trpl proteins form voltage-independent ion channels that can be blocked by Mg^{2+}; however, Trpl channels are neither store-operated nor ion selective, with respect to Na^{+}, Ba^{2+} and Ca^{2+} (18, 29)

The light induced current in the photoreceptors of Trpl$^-$ mutants does not include the transient calcium influx found in both wildtype and Trp$^-$ mutants; yet, Trpl$^-$ mutants display a light response that is not different from that of wildtype. Trp$^-$:Trpl$^-$ double mutants are almost completely unresponsive to light, which indicates the importance of both in Ca^{2+}-influx (15, 36, 41). Further studies indicated that the cellular and molecular characteristics of Trpl suggest that it is a channel protein that is responsible for the early influx of calcium in response to light.

1.3.1b Transducisomes

Since both Trp and Trpl are essential for Ca^{2+} influx in the Drosophila photoreceptor, it is not surprising that they coimmunoprecipitate (15, 36, 41). The resultant heterotetrameric complex appears to involve the direct interaction between their amino-terminal and transmembrane regions, *in vitro*; which mimics the conformation of VOC channels. Trpl has a higher affinity for Trp than it has for other Trpl proteins. Moreover, Trp is 10 times more abundant than Trpl. The two main putative SOC channels found in Drosophila photoreceptors appear to be the Trp-homotetramer and the Trp-Trpl heterotetramer (15, 36, 41).

In addition to binding Trpl, Trp forms a larger signalling complex (transducisome) with at least four other proteins that are important to phototransduction. This supermolecular complex includes the light activated G-protein coupled receptor (rhodopsin), eye PLC encoded by norpA (no receptor

potential A), eye PKC encoded by the inaC (inactivation no afterpotential) locus, and calmodulin (9, 24, 25, 53, 54, 58, 61).

While calmodulin binding sites on the carboxyl terminus of both Trp and Trpl allow for direct interaction with calmodulin (53, 58), Trp associates with PLC, PKC and RH1 via INAD, a protein with five 90 amino acid PDZ domains (9, 61). PDZ domains are protein interaction (or "sticky") motifs that bind a number of ion channels and signalling proteins. InaDP215 mutants (which has a mutation in the third, Trp binding PDZ domain) lack the prolonged depolarizing afterpotential seen in wildtype flies and thus are unable to deactivate the light induced current (9, 13, 61). Trp no longer associates with PLC, RH1 and PKC in inaDP215 mutants, and the spatial distribution of Trp is also disrupted. This information suggests that INAD is the scaffolding protein responsible for the formation of the transducisome.

1.3.1c Channel Regulation

The close proximity of the key proteins involved in generating the light induced Ca^{2+} current may play a major role in the modulation of channel activity. Ca^{2+} has been postulated to be the "diffusable messenger" due to its important role in Trp, Trpl and Trp/Trpl channel modulation. Trpl channels can be activated by Ca^{2+} while Trp and Trp/Trpl channels are inhibited by high levels of Ca^{2+} (67) Since both Trp and Trpl contain calmodulin binding sites, of varying affinities for

calmodulin, on their carboxyl termini, it is likely that Ca^{2+}-calmodulin binding to these sites governs this type of modulation (53, 58).

However, the slow deactivation of the light induced current in inaDP215 mutants points towards the importance of the remaining INAD complexed proteins to channel closing. Although a calmodulin:INAD binding site has not been found, many have suggested that such a binding exists and that it regulates the action of the INAD-bound proteins (24, 54).

Although the phosphoinositide pathway uses IP_3 to release Ca^{2+} from the calciosomes, the other product of PLC mediated hydrolysis of PIP_2 appears to be especially relevant to Trpl, and possibly Trp, activation. The formation of polyunsaturated fatty acids by the action of DAG lipase on DAG opens Trp/Trpl channels (10). This phenomenon describes the early, transient influx of calcium mediated by Trpl to be receptor operated. Trp-mediated Ca^{2+}-entry is slower because it responds to store depletion. Mammalian models have described further mechanisms for the modulation of Trp-derived Ca^{2+} channels.

1.3.2 Mammalian Trps

To date, seven different Trp homologs have been described in mammalian cells (30, 31, 40, 44, 45, 57, 62, 63, 65, 68, 69, 70, 71). Like Trp and Trpl, each mammalian Trp displays its own unique characteristics, in terms of cation specificity, conductance and modulation. It is likely that these Trp homologs

form both homo- and heterotetramers in the plasma membrane, like their *Drosophila* counterparts.

In addition, "sticky" proteins, with PDZ domains, have been described in many mammalian cells which suggests that complexes which parallel the *Drosophila* transducisomes may also exist in mammalian systems (38, 56, 60). Moreover, many different G-protein coupled receptors have been shown to activate mammalian Trp channels (7, 59, 66). Given the endless protein combinations, the mammalian system is extremely complex.

In many ways, the mammalian Trps are similar to those of *Drosophila* (4). Trp isoforms 3, 6 and 7 can be activated by DAG much like *Drosophila* Trpl, while Trp isoforms 1, 2, 4 and 5 appear to be store operated (19). Trp4 and Trp5 derived channels may also be opened directly by both PLC and PKC the latter of which is activated by a receptor tyrosine kinase. This suggests that Trps 4 and 5 can flip-flop between receptor-operated and store-operated Ca^{2+} channel depending on the cell system and its environmental conditions (19). The ionic selctivities of mammalian Trps are generally undetermined and those that have been determined are given as permeability ratios for Ca^{2+} and Na^{2+}. These studies suggest that Trps 1, 3, 6 and 7 are less Ca^{2+}-selective, while Trps 2, 4 and 5 are more Ca^{2+}-selective (19). Additional studies should reveal much more regarding the action of each Trp.

Recent work has provided evidence for the "conformational coupling" of human Trp3 and IP_3R through co-immunoprecipitation and glutathione S-transferase-pulldown experiments (8). They found that a region of the carboxyl

terminus of human Trp3 interacts with two regions of IP3R; F2q and F2g. When bound to the F2g region, Ca^{2+} entry was enhanced, while binding to the F2q region reduced it. Therefore, in addition to releasing Ca^{2+} from the calciosomes, IP_3R interacts directly with Trp channels and modulates their activity much like an "on/off" switch (8, 32).

With the addition of IP_3R-Trp coupling to the transducisome model it is clear that Trp-mediated Ca^{2+} entry is tightly regulated by a system whose components remain in close proximity. The importance of this control is undoubtedly relevant to the roles of Ca^{2+} within the cell.

Previous studies have shown that Trps are differentially expressed in brain and other tissues (5, 14, 34, 37, 42, 48, 52, 55, 64). Trp1 can be found throughout the body, while the remaining Trp isoforms appear to be more tissue specific. This specificity suggests that Trp proteins may play a major role in distinct cellular properties. Trps 1, 3, 4, 5 and 6 but not Trp2 have been found within the brain (30). The association between the specialized functions in each brain region and the distribution of Trp isoforms needs examination.

1.4 Proposed Research

Substantia nigra pars compacta (SNpc) neurons produce dopamine in response to cholinergic stimuli and this stimulation would involve receptor operated Ca^{2+} entry. These dopamine-secreting neurons act as inhibitory transmitters to the caudate nucleus and putamen in the motor pathway causing the

resultant movement to be smooth. The selective destruction of this portion of the SN, which sends dopaminergic neurons to the caudate nucleus and putamen, causes Parkinson's Disease (PD) or paralysis agitans. How this selective destruction is brought about is not understood, although many factors such as age and genetic make-up have been shown to be important. It is also known that there are high levels of oxidative stress and iron in these neurons and these are possibly related to elevated levels of cytosolic Ca^{2+}. As Trp channels, in general, are less selective for Ca2+ and various isoforms of Trp may differ in their selectivity, their distribution in substantia nigra would be important as a step in understanding signal transduction and defects leading to PD. Therefore, I set out to determine the expression of Trp mRNAs in the substantia nigra as compared to the whole brain.

2. Experimental Methods

All chemicals were purchased from standard commercial sources.

2.1 Rat Brain Extraction

The rat brain must be extracted quickly and carefully to avoid tissue damage or cellular degradation. The mature male wistar rat is anesthetized in a bell jar containing 0.5 mL methoxyflurane until movement ceases. Decapitation is performed using a guillotine, and the brain is quickly removed from the skull using sterile instruments and placed on ice. It is sectioned into coronal slices from ventral to dorsal; each approximately 2 mm thick. The substantia nigra are located and removed from the appropriate slices using a number 12 scalpel blade (Lance), placed in a sterile 1.5 mL tube and quick-frozen in liquid nitrogen. The rest of the brain is divided into 24 equal sections, each of which is treated in the same manner. The frozen tubes are then stored at –80°C.

2.2 RNA Isolation and Quantification

This protocol is an adaptation of that described in the manual for TRIzol Reagent™ (GIBCO BRL), a mono-phasic solution of phenol and guanidine isothiocyanate. TRIzol Reagent™ disrupts the plasma membrane and dissolves cellular components while maintaining RNA integrity. Each tube is treated in an

identical manner. Seven whole brain tissue samples were randomly selected to compare with the sample isolated from the substantia nigra of the same rat. Each tube is removed from the –80°C freezer and placed on ice. 200 μL of TRIzol Reagent™ is added and the tissue is fully homogenized using a sterile motorized pestle. Following homogenization, an additional 800 μL of TRIzol Reagent™ is added. The tube is then sonicated on ice in 3 bursts of 35 seconds each at an amplitude setting of 8 in Fisher Scientific 550 Sonic Dismembrator, and then allowed to sit at room temperature for 5 minutes to ensure complete dissociation of nucleoprotein complexes. The homogenate is then centrifuged at 4°C at no greater than 12, 000 X g for 10 minutes. The pellet will contain extracellular membranes, polysaccharides and high molecular weight DNA, the supenate will contain RNA, and the excess fat creates a film at the top of the tube. The supernate is removed to a new tube to which 200 μL of choloroform is added. The tube is shaken vigorously, incubated for 3 minutes at room temperature and then centrifuged at 4°C for 15 minutes at no more than 12, 000 X g. This separates the homogenate into 3 phases: a lower organic phase, the DNA containing interphase and a clear upper phase containing the RNA. The upper phase is removed to a new tube, where the RNA is precipitated out of solution by adding 500 μL of isopropanol to each tube and allowing the tube to sit at -40°C for at least 1 hour. The tube is centrifuged at 4°C for 10 minutes at no more than 12000 X g causing a gel-like pellet to form at the bottom of the tube. The supernatant is completely removed and 250 μL of 75% ethanol is added. The sample is then centrifuged at 4°C for 5 minutes at no more than 7, 500 X g. The ethanol is then

removed and the pellet is allowed to dry for 10 to 15 minutes. The RNA pellet is redissolved in 20 μL of 0.001% DEPC (with, approximately 0.0001% DTT) water by passing it through a pipette tip and incubating at 65°C for 15 minutes.

The RNA was quantified by examining the absorbance at 260 nm in a Beckmann DU 640 spectrophotometer.

The quality of the RNA is tested by measuring the 260/280 absorbance ratio and by examining the clarity of the 18S and 28S bands on a 1% RNase-free agarose gel (1X MOPS, 2.2M Formaldehyde, 0.1% DEPC water) run in 1X MOPS buffer.

2.3 DNase Treatment

Both DNase treatment and RT were preformed using enzymes purchased from by GIBCO BRL. DNase treatment selectively destroys the genomic DNA which may remain following RNA isolation. The treatment contains 1 μg of RNA sample, 1 μL of DNase buffer and 1 μL of amplification grade DNase I and made up to 10 μL with 0.001% DEPC water. The tube is incubated for 15 minutes at room temperature. The DNase reaction is stopped by adding 1 μL of 25 mM EDTA, vortexing briefly and incubating the sample at 65°C for 10 minutes.

2.4 Reverse Transcription

Reverse Transcription (RT) produces cDNA specifically from mRNA by using a primer which binds to its polyA tail. 0.5 μg of oligo-dT primer is added to the DNase treated RNA and the tube is then heated to 70°C for 10 minutes. The tube is then quickfrozen on ice immediately to ensure efficient annealing of the oligo dT-primer. 7 μL of cocktail solution (containing 4 μL of 5X First Strand Buffer, 2 μL of 0.1 M DTT and 1 μL of 10 mM dNTP mix) is added to the tube and is collected at the bottom by quick centrifugation. The tube is incubated at 42°C for 2 minutes after which 1 μL of Superscript II (Gibco BRL) is mixed in by pipetting up and down. The tube is then incubated for 50 minutes at 42°C to allow the RT machinery to produce cDNA from the mRNA. The reaction is inactivated by heating to 70°C for 15 minutes and then cooled to 4°C. RT product was stored at –40°C until use.

2.5 Production of MIMICs for Competitive RT-PCR

Inserting a section of DNA into a plasmid allows for the production of numerous copies by transforming bacterial cells to carry the plasmid. PCR products from composite primer-amplified region of pBluescript plasmid were gel purified using QIAquick Gel Extraction Kit (QIAGEN). The purified products were then cloned using the pCR II-TOPO vector from TOPO TA Cloning Kit (Invitrogen). TOP10F' cells were transformed with this plasmid in SOC medium

and β-mercaptoethanol, and spread on Luria broth plates containing 50 μg/mL ampicillin (TOPO TA Cloning Kit). pUC18 Control DNA was used as a transformation control. Colonies were each picked and cultured overnight in 3 mL of Luria broth liquid medium; containing 50 μg/mL ampicillin. The plasmid DNA was isolated using the QIAprep Spin Miniprep Kit (QIAGEN) and precipitated in 10 μL of 3 M Sodium Acetate and 300 uL of 95% ethanol at – 20°C, overnight. The tube was centrifuged at 13000X g for 15 minutes at 2-8°C. The pellet was then dried and resuspended in 50 μL of ddH_20. Analysis was done via PCR using SP6 and T7 primers, and the specific TRP primers. A positive clone for each TRP was selected and amplified by culturing in 500 mL of Luria broth medium; containing 50 μg/mL ampicillin. Isolation of the resulting large amounts of plasmid DNA is done using the QIAGEN Plasmid Maxi Kit (QIAGEN).

These MIMIC plasmids were quantified by measuring their absorbance at 260 nm by spectrophotometry.

2.6 Polymerase Chain Reaction

Polymerase chain reaction (PCR) is used to amplify, or make numerous copies of a certain region of a target DNA. The general PCR protocol used for all experiments was the same. Here, 0.5 μL of reverse transcripts, 7.5 μL of boiled ddH_2O, 2 μL of 10X Buffer [200 mM Tris-HCl (pH 8.4), 500 mM], 2 μL of 2.5 mM $MgCl_2$, 2 μL of 25 mM dNTP Mix (Perkin Elmer), 2 μL of 10 μM

amplification primer (see Table for pairs of primers) and approximately 1 μL of *AmpliTaq* DNA polymerase (Perkin Elmer) to each tube. The PCR reaction and cycling conditions are 92°C for 30 seconds (denaturation step), 66°C for 90 seconds (annealing step), 72°C for 90 seconds (extension step). Following these cycles the tubes are heated to 72°C for 7 minutes to ensure complete extension of all messages. All PCR reactions were done using a Perkin Elmer Gene Amp PCR System 2400

For the cycle optimization, competitive-PCR and Co-PCR experiments, PCR products were radiolabelled by adding 1.5 μCi of Deoxiadenosine [α-^{33}P] Triphosphate (Amersham Pharmacia Biotech) to the reaction mixture and reducing the amount of water added to each tube, accordingly.

All PCR products were run on 15% polyacrylamide gels at 60 mV; with the exclusion of those destined for gel purification, which were run on low-melt 3% agarose gels (SeaKem and NuSieve). These gels were stained in ethidium bromide to visualize the bands and molecular weight markers.

2.6.1 Target and MIMIC PCR

The protocol shown above was used for all PCR reactions involving Target and MIMIC PCRs. The cycle number used for each of these experiments varied from 25 to 30 cycles. In the case of cycle optimization experiments, PCR was carried out for 23, 26, 29, 32 and 35 cycles for each message.

2.6.2 Competitive-PCR

In competitive-PCR experiments 2 μL of MIMIC plasmid was also added to each tube and the amount of water added was reduced, accordingly. An increasing concentrations of MIMIC plasmid were used for each competitive-PCR experiment. For each message both a broad scale and a fine scale competitive-PCR was run. The dilution series for broad scale competitive-PCR was invariably 20,000 fg, 2000 fg, 200 fg and 20 fg for each messsage. The fine scale competitive-PCR dilution series varied depending upon range determined by broad scale competitive-PCR. The cycle number for each message was chosen based upon cycle optimization PCR experiments.

2.6.3 Co-PCR

In Co-PCR experiments 2 μL of 10 μM amplification primer for both Trp3 and Trp6 were added to each tube and the amount of water added was reduced, accordingly.

2.7 Phosphorimaging

In the cases where PCR products were radiolabelled, the resultant gels were dried using a Biorad Model 583 gel dryer. Once dry these gels were exposed to a Storage Phosphor Screen (Molecular Dynamics) for 4 hours. The

screen was then imaged using a Phosphorimager (Molecular Dynamics) and the resultant data was analyzed using ImageQuant™ software (Molecular Dynamics).

Table 1. Primers used in PCR experiments. All Trp composite primers were made as is shown for Trp3 and their product sizes were all approximately 150 bps.

	Primer Sequence		Product Size	Reference
Trp1	Sense	5'- TGC TGT TGG CTG TGA ATG CAC GCT - 3'	280	*AF061266
	Antisense	5'- ACT TCC AGT TCA CGA GAA TTC CGA -3'		
Trp2	Sense	5'- GAA ACG TTC CAG TTT CTC TTC TGG -3'	220	*AF136401
	Antisense	5'- CTT GGA GCG AGC AAA CTT CCA CTC -3'		
Trp3	Sense	5'- CCT GAG CGA AGT CAC ACT CCC AC -3'	525	(34)
	Antisense	5'- CCA CTC TAC ATC ACT GTC ATC C -3'		
Trp4	Sense	5'- CTC TGC AGA TAT CTC TGG GAA G - 3'	490	*AB008889
	Antisense	5'- AAG CTT TGT TCG AGC AAA TTT CCA -3'		
Trp5	Sense	5'- CTA TGA GAC CAG AGC TAT TGA TG -3'	220	(34)
	Antisense	5'- CTA CCA GGG AGA TGA CGT TGT ATG -3'		
Trp6	Sense	5'- GTG CCA AGT CCA AAG TCC CTG C -3'	305	(34)
	Antisense	5'- CTG GGC CTG CAG TAC GTA TC -3'		
pBlueScript (used to generate Trp MIMICs)				
	Sense	5'-TTA GCA GAG CGA GGT ATG-3'	111	Stratagene
	Antisense	5'-CGA CCT GGT CCT CGG TGT-3'		
Composite Primers used to generate Trp3 MIMIC				
	Sense	5'- CCT GAG CGA AGT CAC ACT CCC ACT TAG CAG AGC GAG GTA TG-3'	156	
	Antisense	5'- CCA CTC TAC ATC ACT GTC ATC CCG ACC TGG TCC TCG GTG T-3'		
G3PDH	Sense	5'-CAC GGT CAA GGC TGA GAA C-3'	671	*AF106860
	Antisense	5'-CGA CCT GGT CCT CGG TGT-3'		
pBlueScript (used to generate G3PDH MIMIC)				
	Sense	5'-ACG ACC TAC ACC GAA CTG-3'	408	Stratagene
	Antisense	5'-CTT CCT CGC TCA CTG ACT C-3'		
Composite Primers used to generate G3PDH MIMIC				
	Sense	5'-CAC GGT CAA GGC TGA GAA CAC GAC CTA CAC CGA ACT G-3'	445	
	Antisense	5'-CGA CCT GGT CCT CGG TGT CTT CCT CGC TCA CTG ACT C-3'		

*Genbank Accession numbers

3. Results.

The goal of these experiments was to determine the expression for different Trp isofroms in the substantia nigra and the whole brain of rat. To this end, cDNAs corresponding to Trps 1 to 6 mRNAs were amplified using RT-PCR. In initial experiments, it was observed that PCR products could be obtained without RT. This led to a modification of the procedure to treat RNA with DNase as described in the Methods. Samples were always checked to ensure that there was no PCR product without RT. Based on the band intensities observed in the PCR experiments, Trps 3 and 6 were selected for further study using competitive RT-PCR and Co-RT-PCR. PCR for a larger number of cycles resulted in products for low expression Trps. Initially, all PCR products, except Trp2, were sequenced to verify their identity. Trp2 was not sequenced since its expression in brain was negligibly low.

3.1 RT-PCR of Trps 1 to 6 and G3PDH.

Fig. 1 shows the bands resulting from an RT-PCR experiment where Trps 1 through 6 and G3PDH were amplified using equal amounts of total RNA isolated from the rat substantia nigra or whole brain. Although the molar ratios for the various bands do not correspond directly to the band intensities because each product has a different molecular weight, both the substantia nigra and the whole brain show predominant expression of Trp3 and Trp6 mRNA over Trps 1, 2, 4 and 5. While Trp6 expression appears to be similar in the substantia nigra and the whole brain, the amount of Trp3 mRNA in the substantia nigra appears to be lower than in the whole

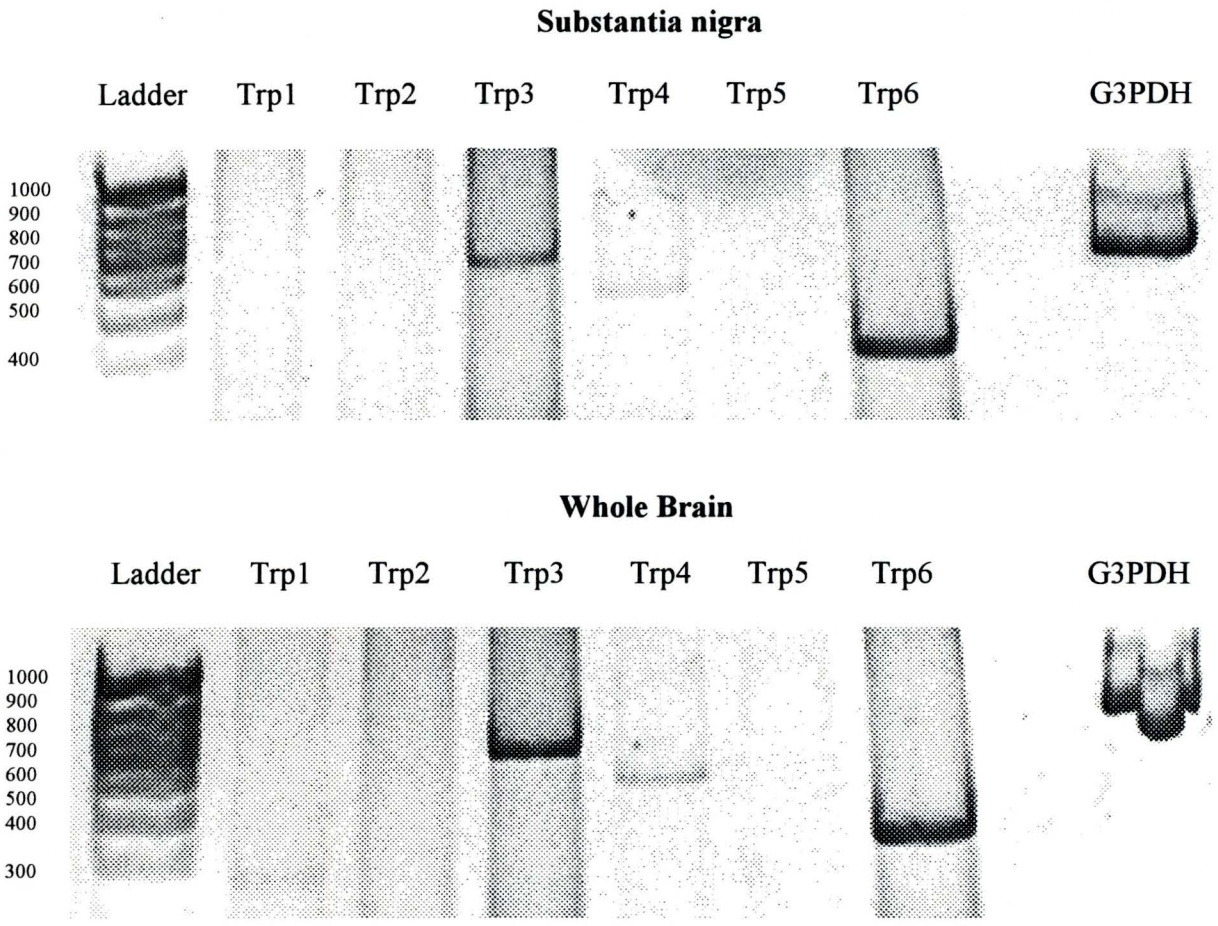

Fig. 1. Ethidium bromide stained gel of RT-PCR products of Trp 1 to 6 and G3PDH mRNA. The reverse transcripts used correspond to 0.025 μg total RNA for substantia nigra or brain. PCR was carried out for 28 cycles. The numbers along the molecular weight ladder are sizes of individual bands in bp. Replicating this experiment in 4 rats gave similar band patterns. See Experimental Methods for details.

brain. This result was consistent in all 4 rats tested even though data for only one is shown in Fig. 1.

Since there is a large variability in PCR, I used competitive RT-PCR to further compare the levels of Trp3 and Trp6 mRNA found in the substantia nigra and the whole brain.

3.2 Competitive RT-PCR for Trp3, Trp6 and G3PDH.

Competitive RT-PCR was used to determine the amount of the Trp3, Trp6 and G3PDH mRNA in the RNA isolated from the substantia nigra or the whole brain. In order to ensure maximum accuracy for competitive RT-PCR, we determined the cycle number at which each message was being amplified at an exponential rate (Figs. 2, 4, and 6). The ratio of the amplified Target to the amplified MIMIC is the same as the initial ratio of Target to MIMIC when amplification efficiencies of the two messages are equal. This occurs during the exponential phase of amplification. The optimum cycle number was determined by amplifiying equal amounts of Target cDNA for an increasing number of cycles. The product cDNA was labelled using ^{33}P-dATP such that plots could be made based on phosphorimage band intensities minus the background in each lane. Each message in both substantia nigra and whole brain was optimized in this manner and Figs. 2, 4 and 6 are examples of the results obtained from all 4 rats. Based on these results, all competitive RT-PCR experiments were performed at 28 cycles.

The molar values of Trp3, Trp6 and G3PDH mRNA were determined in substantia nigra and whole brain using competitive RT-PCR (Figs. 3, 5 and 7). Equal

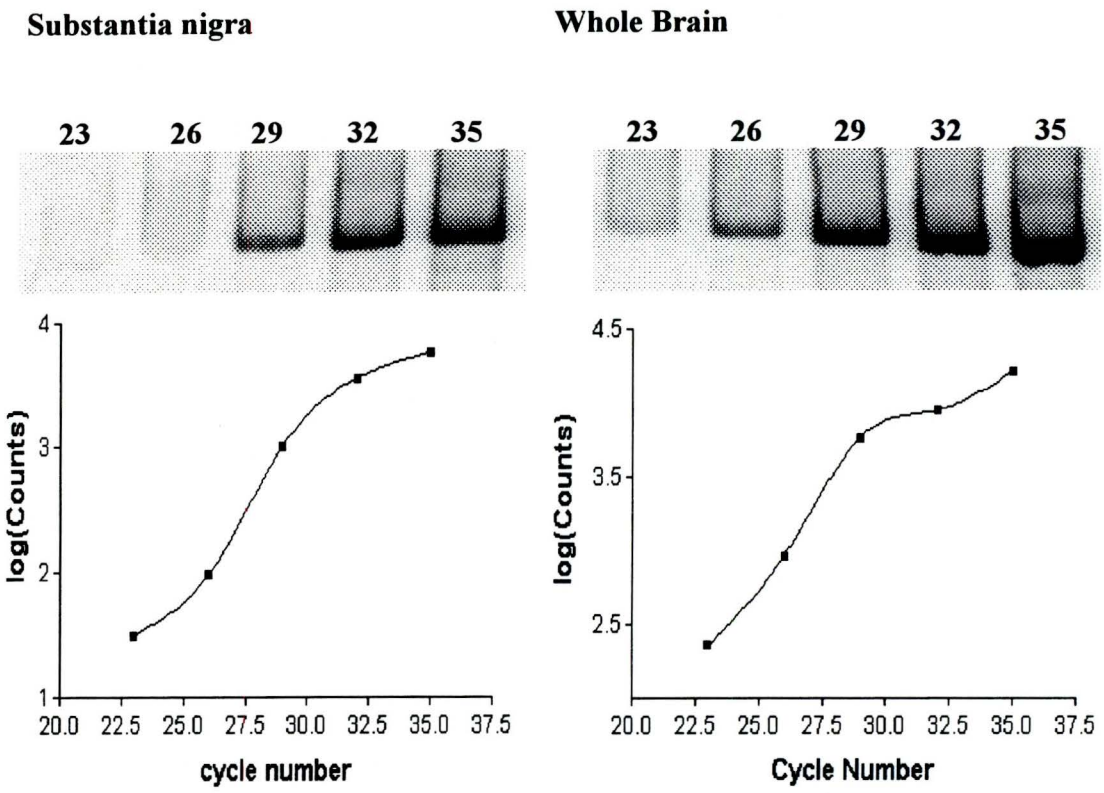

Fig. 2. Phosphorimage showing optimization of cycle number for RT-PCR for Trp3. The reverse transcripts used correspond to 0.025 μg total RNA for substantia nigra or whole brain. The number on top of each lane shows the number of PCR cycles used for amplification. Counts for each band were determined as the average density in the band minus the average density of background in the same lane. In each of the 4 rats used, 28 cycles were considered to be optimum and used in subsequent experiments. See Experimental Methods for details.

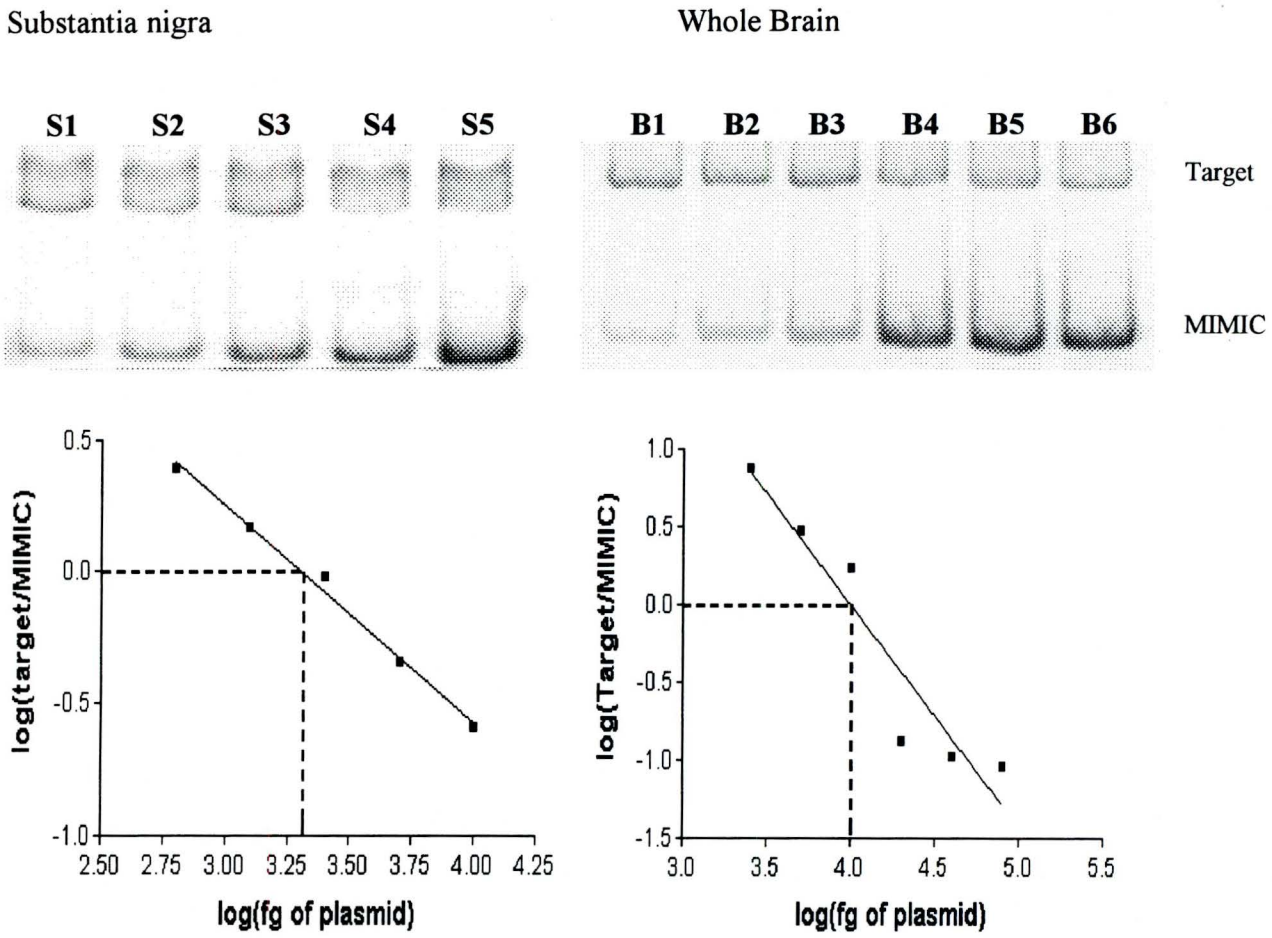

Fig. 3. Phosphorimage showing competitive RT-PCR for Trp3. The reverse transcripts for the target correspond to 0.025 μg total RNA for substantia nigra or whole brain. For the substantia nigra gel, the amounts of MIMIC used in fg were: S1 (625), S2 (1250), S3 (2500), S4 (5000), S5 (10000) and for the whole brain these were B1(2500), B2 (5000), B3 (10000), B4 (20000), B5 (40000) and B6 (80000). The graphs show that in substantia nigra the intensities of the target and mimic were equal when log of MIMIC in fg was 3.30. Since ^{33}P-labelled dATP was used for the quantification, we did the following computation. Trp3 target band contains 276.5 A/T, MIMIC contains 66.5 A/T, trp3 plasmid = 4106 bp,1 bp = 660 Da and the amount of total RNA = 0.025 μg, we compute a value of 0.0071 trp3 fmol/μg substantia nigra RNA. For the whole brain the intensities of the target and MIMIC were equal when log of MIMIC in fg was 3.994 thus giving a value of 0.035 trp3 fmol/μg whole brain RNA. The experiments were replicated in 4 rats and the resulting values are in Fig. 8. See Experimental Methods for details.

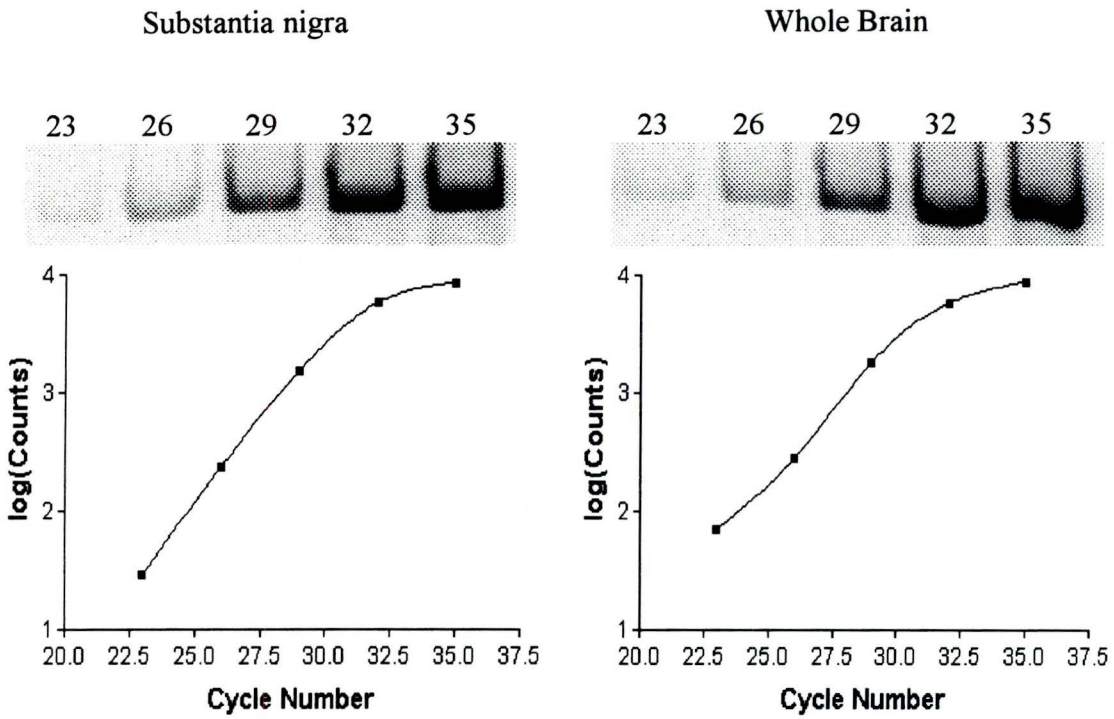

Fig. 4. Phosphorimage showing optimization of cycle number for RT-PCR for Trp6. The reverse transcripts used correspond to 0.025 μg total RNA for substantia nigra or whole brain. The number on top of each lane shows the number of PCR cycles used for amplification. Counts for each band were determined as the average density in the band minus the average density of background in the same lane. In each of the 4 rats used, 28 cycles were considered to be optimum and used in subsequent experiments. See Experimental Methods for details.

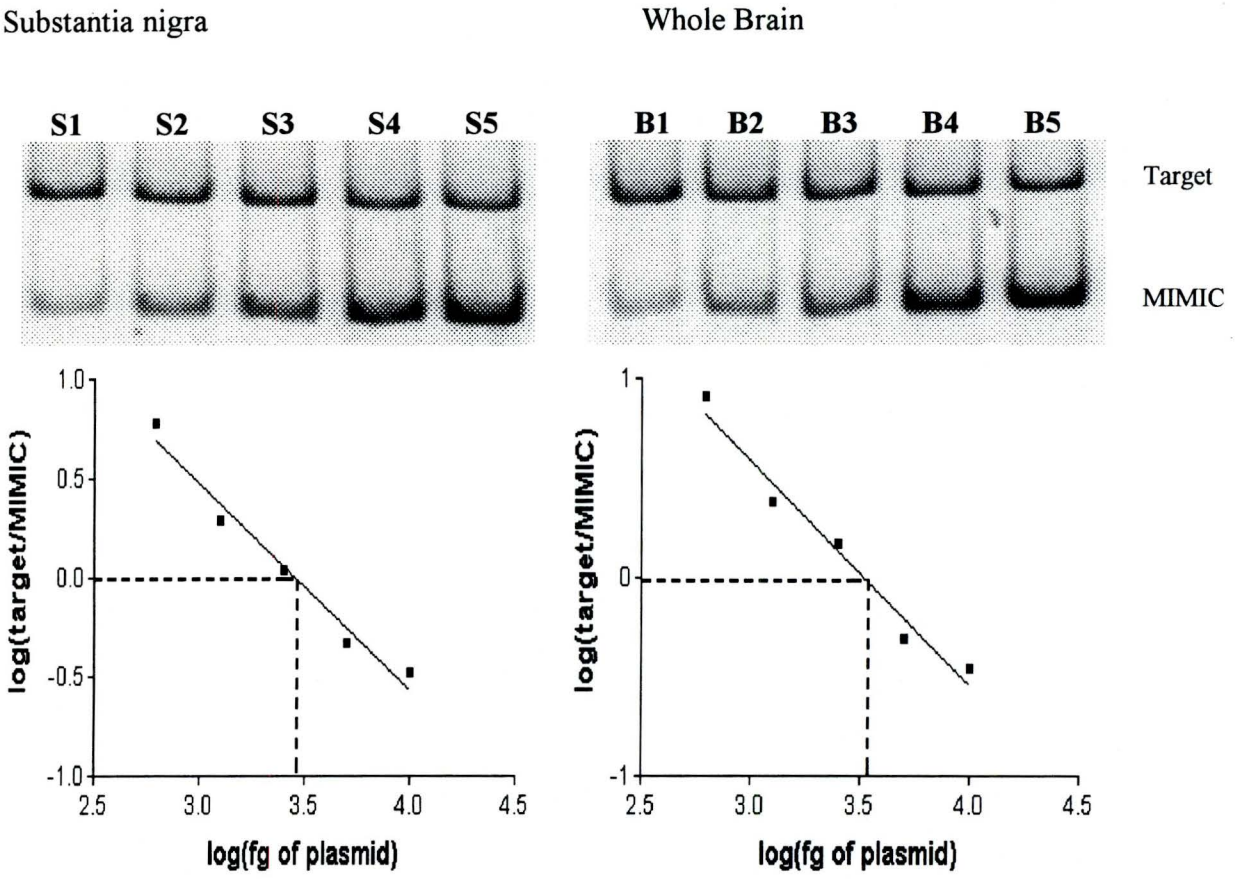

Fig. 5. Phosphorimage showing competitive RT-PCR for Trp6. The reverse transcripts for the target correspond to 0.025 μg total RNA for substantia nigra or whole brain. For the substantia nigra gel, the amounts of MIMIC used in fg were: S1 (625), S2 (1250), S3 (2500), S4 (5000) and S5 (10000), and for the whole brain these were B1(625), B2 (1250), B3 (2500), B4 (5000) and B5 (10000). The graphs show that in substantia nigra the intensities of the target and mimic were equal when log of MIMIC in fg was 3.452. Since ^{33}P-labelled dATP was used for the quantification, we did the following computation. G3PDH target band contains 180.5 A/T, MIMIC contains 66.5 A/T, G3PDH plasmid = 4103 bp,1 bp = 660 Da and the amount of total RNA = 0.025 μg, we compute a value of 0.015 G3PDH fmol/μg substantia nigra RNA. For the whole brain the intensities of the target and MIMIC were equal when log of MIMIC in fg was 3.514 thus giving a value of 0.017 trp3 fmol/μg whole brain RNA. The experiments were replicated in 4 rats and the resulting values are in Fig. 8. See Experimental Methods for details.

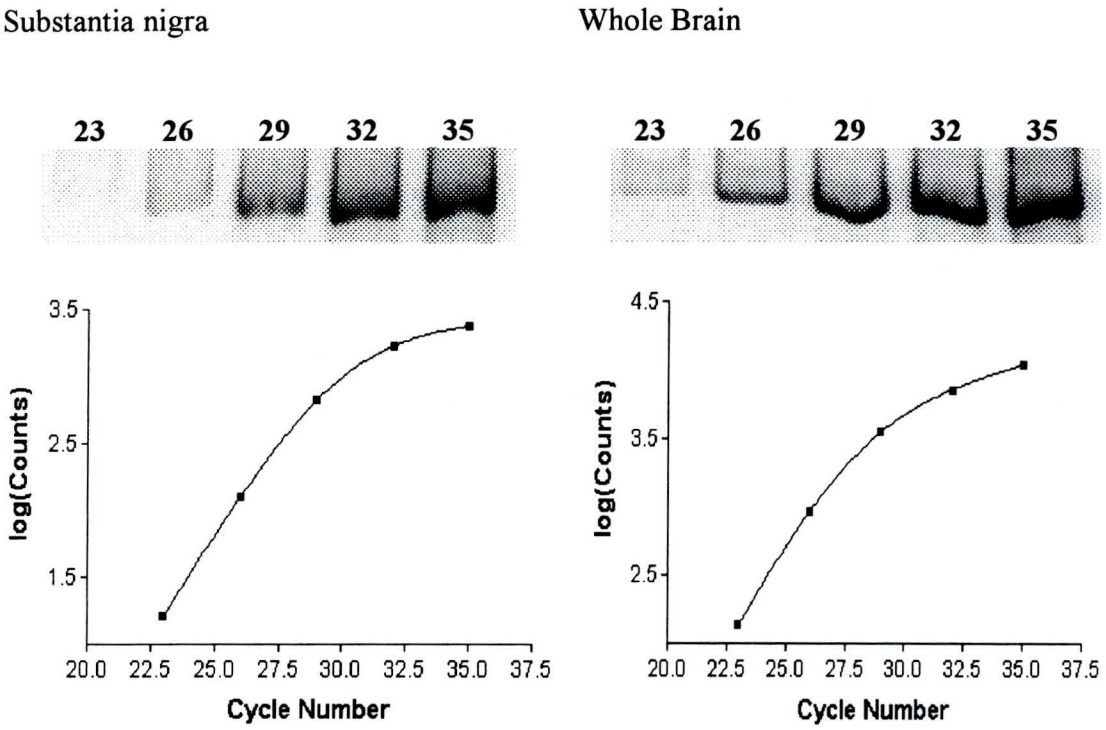

Fig. 6. Phosphorimage showing optimization of cycle number for RT-PCR for G3PDH. The reverse transcripts used correspond to 0.025 μg total RNA for substantia nigra or whole brain. The number on top of each lane shows the number of PCR cycles used for amplification. Counts for each band were determined as the average density in the band minus the average density of background in the same lane. In each of the 4 rats used, 28 cycles were considered to be optimum and used in subsequent experiments. See Experimental Methods for details.

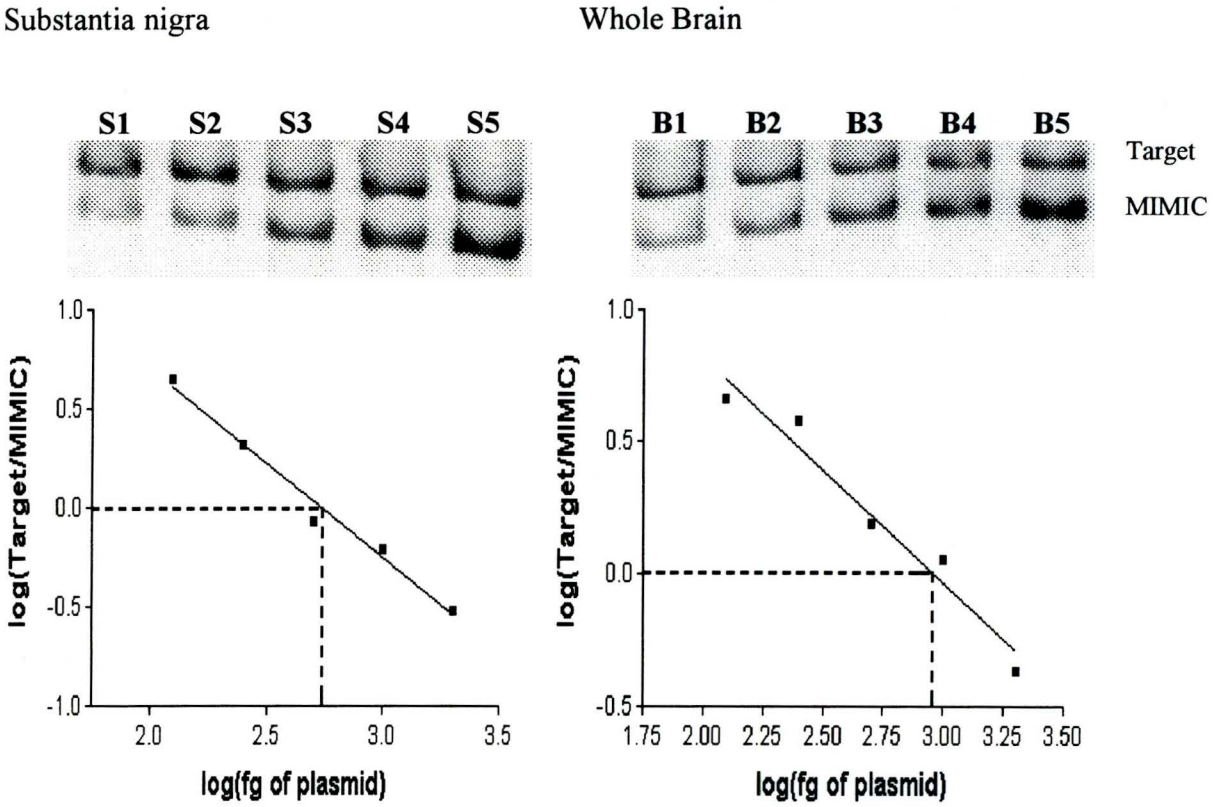

Fig. 7. Phosphorimage showing competitive RT-PCR for G3PDH. The reverse transcripts for the target correspond to 0.025 μg total RNA for substantia nigra or whole brain. For the substantia nigra gel, the amounts of MIMIC used in fg were: S1 (125), S2 (250), S3 (500), S4 (1000), S5 (2000) and for the whole brain these were B1(125), B2 (250), B3 (5000), B4 (1000) and B5 (2000). The graphs show that in substantia nigra the intensities of the target and mimic were equal when log of MIMIC in fg was 2.73. Since ^{33}P-labelled dATP was used for the quantification, we did the following computation. G3PDH target band contains 284.5 A/T, MIMIC contains 184.5 A/T, G3PDH plasmid = 4396 bp,1 bp = 660 Da and the amount of total RNA = 0.025 μg, we compute a value of 0.0048 G3PDH fmol/μg substantia nigra RNA. For the whole brain the intensities of the target and MIMIC were equal when log of MIMIC in fg was 2.957 thus giving a value of 0.0081 G3PDH fmol/μg whole brain RNA. The experiments were replicated in 4 rats and the resulting values are in Fig. 8. See Experimental Methods for details.

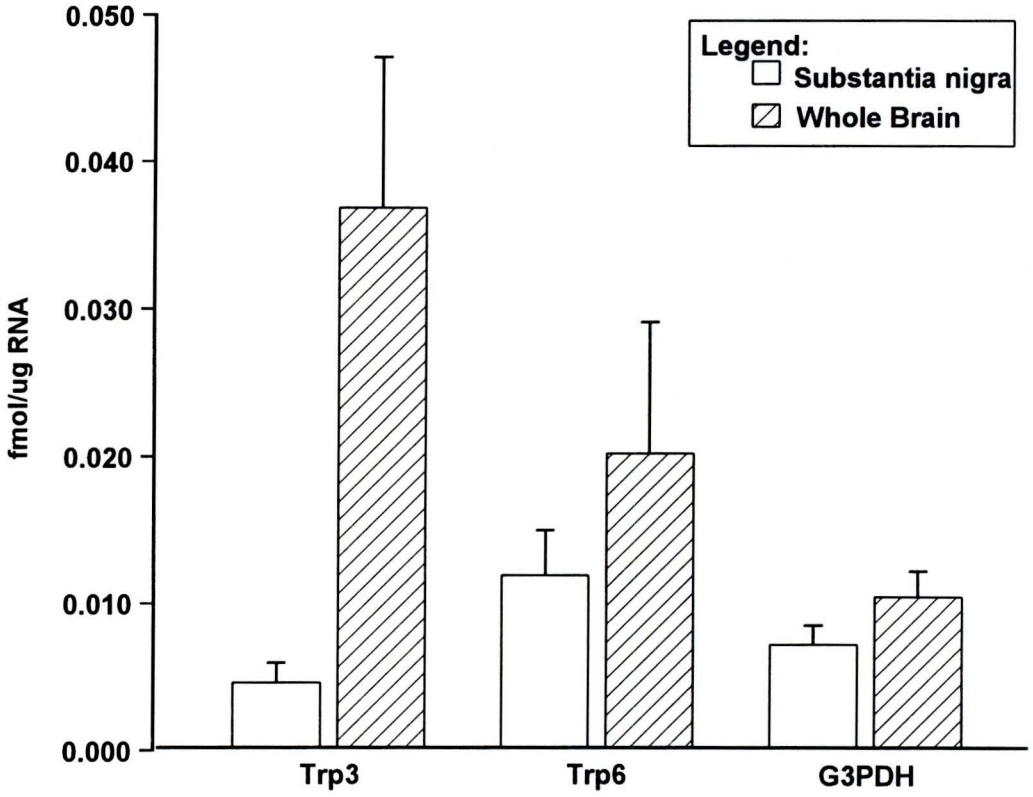

Fig. 8. Comparison of Trp3, 6 and G3PDH mRNA values in competitive RT-PCR experiments. The values shown are mean ± SEM from 4 rats as shown in Figs. 3, 5 and 7. Only the values for trp3 were significantly different between substantia nigra and whole brain ($p < 0.05$).

amounts of Target cDNA were competed against increasing amounts of MIMIC DNA during PCR amplification. As with the cycle optimization experiments, the product cDNAs were labeled using ^{33}P-dATP.

Phosphorimages of the resulting gels were analyzed by measuring the band intensities and subtracting the background found in each lane. The point at which the band intensity of the Target was equal to that of the MIMIC was determined by ploting the log ratio of Target to MIMIC in each lane against the log of the initial plasmid added to the corresponding PCR tube. Examples of these log-log plots can be found in Figs. 3, 5 and 7. In each case, the x-intercept corresponds to the uncorrected initial amount of Target cDNA. These values were corrected for molecular weights and AT compositions because ^{33}P-dATP incorporations were used for the quantification (see Experimental Methods).

Fig. 8 gives the mean ± SEM of the competitive RT-PCR data obtained for each message over 4 rats. The mean level of Trp3 is 0.0046 ± 0.0011 fmol/μg RNA in the substantia nigra and 0.0368 ± 0.0089 fmol/μg RNA in the whole brain, indicating that Trp3 expression in the substantia nigra is only 12% of that in the whole brain ($p<0.05$). The mean level of Trp6 is 0.012 ± 0.0027 fmol/μg RNA in the substantia nigra and 0.020 ± 0.0077 fmol/μg RNA in the whole brain, indicating that Trp6 expression does not differ significantly in the substantia nigra and the whole brain ($p>0.05$). The mean level of G3PDH was not significantly different in substantia nigra and the whole brain ($p>0.05$) with mean levels of 0.0072 ± 0.0011 fmol/μg RNA and 0.010 ± 0.0015 fmol/μg RNA, respectively.

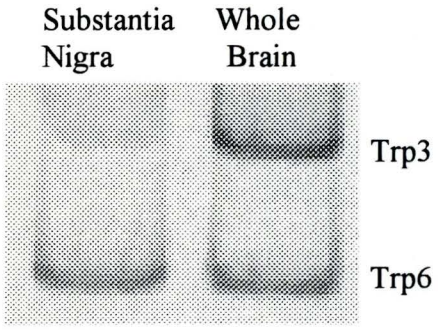

Fig. 9. Co-RT-PCR of Trp3 and Trp6 in substantia nigra and whole brain. The experiment was conducted as in Fig. 3 except that primers for both Trp3 and Trp6 were used together and amplificaiton was carried out for only 26 cycles. Replicating the experiment in 4 rats consistently gave the result that Trp3 mRNA was less abundant in the substantia nigra than in the whole brain and that the expression of Trp6 mRNA in the two tissues was similar.

The results obtained from competitive RT-PCR show that expression of Trp6 mRNA is similar in the substantia nigra and whole brain, while the amount of Trp3 mRNA in the substantia nigra is lower than in the whole brain.

3.3 Co-RT-PCR of Trp3 and Trp6.

To ensure that Trp3 mRNA expression was indeed lower in the substantia nigra than in the whole brain and that this result was not a phenomenon of the competitive RT-PCR procedure, I validated my results using Co-RT-PCR. Here, equal amounts of total RNA from substantia nigra and whole brain were each amplified using both Trp3 and Trp6 primers in the same tube. Again, the PCR product was labelled using ^{33}P-dATP such that the resultant bands could be analyzed using the phosphorimager. The band intensities observed in Fig. 9 are representative of those observed for all 4 rats. The mean ratio of Trp3 to Trp6 was 0.25 ± 0.011 in substantia nigra and 1.25 ± 0.16 in the whole brain. The results from Co-RT-PCR confirm that the level of Trp3 is significantly lower in the substantia nigra than in the whole brain ($p<0.05$).

4. Discussion

Based on competitive RT-PCR studies, I found that the substantia nigra mainly expresses Trp3 and Trp6 mRNA, yet Trp3 mRNA is 8 times more abundant in the whole brain than in the substantia nigra. The discussion will outline the pros and cons of the methods used. However, the focus will be on the possible interpretations of these results in terms of cellular expression and functional relevance.

4.1 Validity of Method Used

During this set of experiments I isolated mRNA from rat brain tissue and used competitive RT-PCR and Co-RT-PCR to compare the levels of Trp 3 and Trp6 mRNA expression in the substantia nigra to those found in the whole brain. Each aspect of this experiment will be examined.

4.1.1 Animal Model

Rats were chosen as the animal model to be used because a Parkinsonian rat behavioral model already exists. Rats which have been injected with either 6-hydroxydopamine, N-methyl-4-phenyl-1,2,3,6-tetrahydropyridine or iron show distict motor abnormalities in conjunction with dopaminergic cell-specific degeneration in the substantia nigra. Although these behavioral changes are not identical to those observed in human Parkinson's Disease, this model is generally accepted (2, 27). There has also been significant work in other aspects of rat brain and furthermore the

size of the brain and the ready availability of the animal makes it easy to dissect the substantia nigra. The substantia nigra is easily located in coronal sections based on its position relative to the pons and is distinguished based on its "cat-eye"-like appearance.

4.1.2 RNA Isolation

Several methods were initially tested to optimize the recovery of good quality total RNA before arriving at the methods used. In total RNA, ribosomal RNA is the major species and the subunits 28S and 18S of ribosomal RNA are equimolar. The presence of a bright 4.7 kb band and a lighter 1.9 kb band in ethidium bromide stained gel is a measure of intactness of RNA. This criterion along with the measurement of the 260/280 nm absorbance ratio, indicate that this method reproducibly gave me good quality RNA.

4.1.3 Quantification

The substantia nigra and the whole brain tissues are not homogeneous, therefore the total RNA isolated was not strictly derived from neuronal cells.

The results obtained using total RNA were normalized in competitive RT-PCR through parallel experiments on G3PDH mRNA in the same tissues. Furthermore, these results were internally verified by Co-RT-PCR of Trp3 and Trp6 mRNA messages.

Various methods for the quantification of mRNA levels within brain tissue were examined prior to choosing competitive RT-PCR for use in this study. *In situ* hybridization has been used to determine Trp6 mRNA distribution in rat brain tissue, yet the limited sequence data for the remaining rat Trp mRNA messages made the generation of probes difficult. Northern blot analysis requires a large amount of total RNA to sense less abundant mRNA messages and, therefore, was not appropriate for my study of the total RNA isolated from the substantia nigra tissue of individual rats. RNase protection assays were not used due, again, to limited Trp mRNA sequence data required to develop probes.

Competitive RT-PCR is a quantitative method that uses the sensitivity of RT-PCR to derive semi-quantitative data on rare mRNAs in small amounts of tissue (6, 16, 20, 39, 51). Furthermore, Trp mRNA sequence data was not required for competitive RT-PCR because previous studies had designed primer sets for RT-PCR experiments in rat brain.

The reliability of competitive RT-PCR depends upon amplification efficiency. That is, the ratio of the amplified Target to the amplified MIMIC is the same as the initial ratio of Target to MIMIC when amplification efficiencies of the two messages are equal. Although, in theory, RT-competitive-PCR can be accurate once the PCR reactions plateau, in practice the most accurate results are always acquired during the exponential phase. Thus, cycle optimization was necessary. Furthermore, amplification efficiency requires that primer affinity, melt time, and extension time must be optimized for each competitive RT-PCR experiment. Since both target and MIMIC cDNA sequences recognize the primer sequences equally, the annealing

temperature and time was identical for each set. The target and MIMIC PCR products differ in length by no more than 300 bp, therefore their melt times were not different. Moreover, using a long melting time may reduce the efficiency of DNA polymerase. Finally, a long extension time was used to reduce the risk of an incomplete reaction.

Tube-to-tube variation during the RT-competitive-PCR step was unavoidable, yet, it was the plot derived from amplified target to amplified MIMIC ratios determined for each tube which allows for quantification of the target mRNA. In this way, the error associated with tube-to-tube variation becomes negligible.

The efficiency of synthesizing cDNA from total RNA is not the same for all mRNA messages since secondary structure plays a major role in reverse trascriptase efficiency. Although this may be the case, this does not negate the fact that Trp3 mRNA expression is lower in the substantia nigra than in the whole brain. Furthermore, the similar expression of both Trp6 and G3PDH mRNAs in these same tissues in all 4 rats suggests that the efficiency of reverse trascriptase was not tissue dependent.

4.1.4 Co-RT-PCR

Co-RT-PCR was used to verify those results produced by competitive RT-PCR. Like competitive RT-PCR, the amplification efficiency of both messages must be optimized (43). Since Co-RT-PCR requires the addition of higher primer concentrations than in competitive RT-PCR, the cycle number was reduced in order

to ensure that both Trp3 and Trp6 products were within the exponential phase when they were analyzed (43).

4.2 Significance of Trp3 and Trp6 Expression

Previous studies show that Trps are differentially expressed in brain and other tissues. While Trp1 is ubiquitous, Trp isoforms 3, 4, 5 and 6 are preferentially expressed in brain and Trp2 expression is thought to be limited to the vomeronasal organ and the testis (5, 14, 31, 34, 37, 40, 42, 46, 48, 52, 55, 64). My results are consistent with an earlier study that used RT-PCR to show that the brain expresses Trp3 and Trp6 mRNAs (34). In the same study, RT-PCR and *in situ* hybridization studies revealed that Trp6 mRNA is preferentially expressed in the hippocampal dentate gyrus and cortical layers II and III (34). I have shown that substantia nigra also expresses Trp6 mRNA at high levels relative to the other Trp mRNA messages.

Beyond my own findings, Trp7 is the only other Trp isoform known to be expressed in the substantia nigra (40). Although the level of Trp7 mRNA is low, this result is interesting since Trp isoforms 3, 6, and 7 are thought to be part of a subgroup of Trp isoforms, which display store depletion independent regulation and have similar cation specificities (19). We did not perform any experiments with Trp7 because it was not discovered until very recently, and because the data in rat is still very limited.

A model for the organization of Trp proteins into channels has been described (70), and suggests that 4 Trp proteins come together to form a multimeric cation

channel. The Trp protein composition of these channels depends upon the amounts of each specific Trp protein available within the cell. When one Trp protein is more prevalent within the cell it will be preferentially incorporated into the channel. Therefore, the specific Trp mRNA distributions within the body suggest that the resultant Trp proteins may be related to specific cellular properties. Since I have shown that Trp3 mRNA is present at lower levels in the substantia nigra than in the whole brain, it follows thatTrp3 protein is less likely to be included in Trp cation channels. Moreover, Trp6 protein will be preferentially incorporated into these channels in the substantia nigra.

Although much work has been geared towards determining the cation specificity of Trp channels, the results have varied depending on the organism, the cell type chosen for expression and the lab performing the experiments. On the whole, there is close similarity between Trp3, Trp6 and Trp7, and between Trp4 and Trp5. Although the expression of each of these Trp cDNAs in different mammalian cell lines has yeilded Ca^{2+}-permeable nonselective cation channels which are activated downstream of G-protein coupled receptor activation, in the cases of Trp3, Trp6 and Trp7 this activation has been shown to be store depletion independent. Experiments show that all three are operated by DAGs in a membrane-delimited, PKC-independent fashion (23). This said, two reports have shown either increased Ca^{2+} entry or Ca^{2+} currents after store depletion in cells transfected with the Trp3 cDNA. Other reports have indicated that Trp3 can be activated through conformation coupling with IP_3 receptor or can be activated directly by IP_3, and not by store depletion (12, 17). One report has shown that when Trp3 is present at low levels,

Trp3 is tightly bound to the IP3 receptor which prevents activation by DAG (28). Conversely, when Trp3 is highly expressed, the Trp3 channels are thought to outnumber the IP_3 receptors, which leaves the channels susceptable to lipid messengers. In this way, a reduction in the levels of Trp3 mRNA in the substantia nigra might not only lead to a reduction in Trp3 incorporation in to Trp Ca^{2+} channels but may also cause those channels containing Trp3 to be inactive.

Neuronal tissues have lower densities of ER Ca^{2+} pump (33) but have been reported to contain large amounts of Ca^{2+} buffering proteins such as parvalbumin, calretinin, calbindin, calcineurin, and S100α (21). To this end, a study relating the distribution of SERCA2 in rat brain tissue to $^{45}Ca^{2+}$ uptake found that the substantia nigra, in particular, displayed extremely low levels of SERCA2 while showing high levels of $^{45}Ca^{2+}$ (33). This finding corresponds to the receptor-operated Ca^{2+} entry in neuronal cells being associated more with DAG and IP_3 than with store depletion.

4.3 Future

The finding that Trp3 mRNA is less abundant in the substantia nigra than in the whole brain suggests that the Trps found within specific cell types play a role in the cellular operations. Unfortunately, data pertaining to mammalian Trp protein channels characteristics is limited to the homotetrameric variety (19, 26). Since it is most likely that heterotetrameric, rather than homotetrameric, Trp protein channels are the prevalent in mammalian cells, an understanding of these more complex

channels may improve our understanding of the importance of Trp distribution to cellular and tissue function.

Moreover, the ionic selectivity of homotetrameric Trp protein channels are given in terms of the permeability ratio of Ca^{2+} to Na^{+}. Although Mn^{2+} has been shown to enter the cell through receptor operated Ca^{2+} channels, the permeability of Trp protein channels to the divalent cations, such as transition metals, remains unknown. Furthermore, Trp has been linked to oxidative stress (1) which is though to be the main cause of neurodegeneration. Whether iron entry through Trp6 in the substantia nigra neurons is a source of neurotoxicity which leads to Parkinson's Disease remains to be explored.

5. References

1. **Balzer, M., B. Lintschinger, and K. Groschner.** Evidence for a role of Trp proteins in the oxidative stress-induced membrane conductances of porcine aortic endothelial cells. *Cardiovasc.Res.* 42: 543-549, 1999.

2. **Ben-Shachar, D., G. Eshel, P. Riederer, and M.B. Youdim.** Role of iron and iron chelation in dopaminergic-induced neurodegeneration: implication for Parkinson's disease. *Ann.Neurol.* 32 Suppl: S105-S1101992.

3. **Berridge, M.J.** Inositol trisphosphate and calcium signalling. *Nature* 361: 315-325, 1993.

4. **Birnbaumer, L., X. Zhu, M. Jiang, G. Boulay, M. Peyton, B. Vannier, D. Brown, D. Platano, H. Sadeghi, E. Stefani, and M. Birnbaumer.** On the molecular basis and regulation of cellular capacitative calcium entry: roles for Trp proteins. *Proc.Natl.Acad.Sci.U.S.A.* 93: 15195-15202, 1996.

5. **Bobanovic, L.K., M. Laine, C.C. Petersen, D.L. Bennett, M.J. Berridge, P. Lipp, S.J. Ripley, and M.D. Bootman.** Molecular cloning and immunolocalization of a novel vertebrate trp homologue from Xenopus. *Biochem.J* 340 (Pt 3): 593-599, 1999.

6. **Bouaboula, M., P. Legoux, B. Pessegue, B. Delpech, X. Dumont, M. Piechaczyk, P. Casellas, and D. Shire.** Standardization of mRNA titration

using a polymerase chain reaction method involving co-amplification with a multispecific internal control. *J Biol.Chem.* 267: 21830-21838, 1992.

7. **Boulay, G., X. Zhu, M. Peyton, M. Jiang, R. Hurst, E. Stefani, and L. Birnbaumer.** Cloning and expression of a novel mammalian homolog of Drosophila transient receptor potential (Trp) involved in calcium entry secondary to activation of receptors coupled by the Gq class of G protein. *J Biol.Chem.* 272: 29672-29680, 1997.

8. **Boulay, G., D.M. Brown, N. Qin, M. Jiang, A. Dietrich, M.X. Zhu, Z. Chen, M. Birnbaumer, K. Mikoshiba, and L. Birnbaumer.** Modulation of Ca(2+) entry by polypeptides of the inositol 1,4, 5-trisphosphate receptor (IP3R) that bind transient receptor potential (TRP): evidence for roles of TRP and IP3R in store depletion-activated Ca(2+) entry [see comments]. *Proc.Natl.Acad.Sci.U.S.A.* 96: 14955-14960, 1999.

9. **Chevesich, J., A.J. Kreuz, and C. Montell.** Requirement for the PDZ domain protein, INAD, for localization of the TRP store-operated channel to a signaling complex. *Neuron* 18: 95-105, 1997.

10. **Chyb, S., P. Raghu, and R.C. Hardie.** Polyunsaturated fatty acids activate the Drosophila light-sensitive channels TRP and TRPL. *Nature* 397: 255-259, 1999.

11. **Cook, B. and B. Minke.** TRP and calcium stores in Drosophila phototransduction. *Cell Calcium* 25: 161-171, 1999.

12. **Dong, Y., D.L. Kunze, L. Vaca, and W.P. Schilling.** Ins(1,4,5)P3 activates Drosophila cation channel Trpl in recombinant baculovirus-infected Sf9 insect cells. *Am.J Physiol.* 269: C1332-C13391995.

13. **Estacion, M., W.G. Sinkins, and W.P. Schilling.** Stimulation of Drosophila TrpL by capacitative Ca2+ entry. *Biochem.J* 341 (Pt 1): 41-49, 1999.

14. **Funayama, M., K. Goto, and H. Kondo.** Cloning and expression localization of cDNA for rat homolog of TRP protein, a possible store-operated calcium (Ca2+) channel. *Brain Res.Mol.Brain Res.* 43: 259-266, 1996.

15. **Gillo, B., I. Chorna, H. Cohen, B. Cook, I. Manistersky, M. Chorev, A. Arnon, J.A. Pollock, Z. Selinger, and B. Minke.** Coexpression of Drosophila TRP and TRP-like proteins in Xenopus oocytes reconstitutes capacitative Ca2+ entry. *Proc.Natl.Acad.Sci.U.S.A.* 93: 14146-14151, 1996.

16. **Haberhausen, G., J. Pinsl, C.C. Kuhn, and C. Markert-Hahn.** Comparative study of different standardization concepts in quantitative competitive reverse transcription-PCR assays. *J Clin.Microbiol.* 36: 628-633, 1998.

17. **Hardie, R.C. and B. Minke.** Novel Ca2+ channels underlying transduction in Drosophila photoreceptors: implications for phosphoinositide-mediated Ca2+ mobilization. *Trends.Neurosci.* 16: 371-376, 1993.

18. **Hardie, R.C., H. Reuss, S.J. Lansdell, and N.S. Millar.** Functional equivalence of native light-sensitive channels in the Drosophila trp301 mutant and TRPL

cation channels expressed in a stably transfected Drosophila cell line. *Cell Calcium* 21: 431-440, 1997.

19. **Harteneck, C., T.D. Plant, and G. Schultz.** From worm to man: three subfamilies of TRP channels. *Trends.Neurosci.2000.Apr.;23.(4.):159.-66.* 23: 159-166, 2000.

20. **Hayward, A.L., P.J. Oefner, S. Sabatini, D.B. Kainer, C.A. Hinojos, and P.A. Doris.** Modeling and analysis of competitive RT-PCR. *Nucleic.Acids.Res.* 26: 2511-2518, 1998.

21. **Heizmann, C.W. and K. Braun.** Changes in Ca(2+)-binding proteins in human neurodegenerative disorders. *Trends.Neurosci.* 15: 259-264, 1992.

22. **Hirsch, E.C. and B.A. Faucheux.** Iron metabolism and Parkinson's disease. *Mov.Disord.* 13 Suppl 1: 39-45, 1998.

23. **Hofmann, T., A.G. Obukhov, M. Schaefer, C. Harteneck, T. Gudermann, and G. Schultz.** Direct activation of human TRPC6 and TRPC3 channels by diacylglycerol. *Nature* 397: 259-263, 1999.

23A. **Holda, J.R., A. Klishin, M. Sedova, J. Huser, and L.A. Blatter.** Capacitative Calcium Entry. NIPS 13: 157-163, 1998.

24. **Huber, A., P. Sander, and R. Paulsen.** Phosphorylation of the InaD gene product, a photoreceptor membrane protein required for recovery of visual excitation. *J.Biol.Chem.* 271: 11710-11717, 1996.

25. **Huber, A., P. Sander, A. Gobert, M. Bahner, R. Hermann, and R. Paulsen.** The transient receptor potential protein (Trp), a putative store- operated Ca2+ channel essential for phosphoinositide-mediated photoreception, forms a signaling complex with NorpA, InaC and InaD. *EMBO J.* 15: 7036-7045, 1996.

26. **Hurst, R.S., X. Zhu, G. Boulay, L. Birnbaumer, and E. Stefani.** Ionic currents underlying HTRP3 mediated agonist-dependent Ca2+ influx in stably transfected HEK293 cells. *FEBS Lett.* 422: 333-338, 1998.

27. **Jellinger, K.A.** The role of iron in neurodegeneration: prospects for pharmacotherapy of Parkinson's disease. *Drugs Aging* 14: 115-140, 1999.

28. **Kiselyov, K. and S. Muallem.** Fatty acids, diacylglycerol, Ins(1,4,5)P3 receptors and Ca2+ influx. *Trends.Neurosci.* 22: 334-337, 1999.

29. **Kunze, D.L., W.G. Sinkins, L. Vaca, and W.P. Schilling.** Properties of single Drosophila Trpl channels expressed in Sf9 insect cells. *Am.J Physiol.* 272: C27-C341997.

30. **Liman, E.R., D.P. Corey, and C. Dulac.** TRP2: a candidate transduction channel for mammalian pheromone sensory signaling. *Proc.Natl.Acad.Sci.U.S.A.* 96: 5791-5796, 1999.

31. **Liu, X., W. Wang, B.B. Singh, T. Lockwich, J. Jadlowiec, B. O'Connell, R. Wellner, M.X. Zhu, and I.S. Ambudkar.** Trp1, a candidate protein for the store-operated Ca(2+) influx mechanism in salivary gland cells [published

erratum appears in J Biol Chem 2000 Mar 31;275(13):9890-1]. *J Biol.Chem.2000.Feb.4.;275.(5.):3403.-11.* 275: 3403-3411, 2000.

32. **Ma, H.T., R.L. Patterson, D.B. van Rossum, L. Birnbaumer, K. Mikoshiba, and D.L. Gill.** Requirement of the inositol trisphosphate receptor for activation of store-operated Ca2+ channels [see comments]. *Science 2000.Mar.3.;287.(5458.):1647.-51.* 287: 1647-1651, 2000.

33. **Miller, K.K., A. Verma, S.H. Snyder, and C.A. Ross.** Localization of an endoplasmic reticulum calcium ATPase mRNA in rat brain by in situ hybridization. *Neuroscience* 43: 1-9, 1991.

34. **Mizuno, N., S. Kitayama, Y. Saishin, S. Shimada, K. Morita, C. Mitsuhata, H. Kurihara, and T. Dohi.** Molecular cloning and characterization of rat trp homologues from brain. *Brain Res.Mol.Brain Res.* 64: 41-51, 1999.

35. **Montell, C. and G.M. Rubin.** Molecular characterization of the Drosophila trp locus: a putative integral membrane protein required for phototransduction. *Neuron* 2: 1313-1323, 1989.

36. **Montell, C.** New light on TRP and TRPL. *Mol.Pharmacol.* 52: 755-763, 1997.

37. **Moore, T.M., G.H. Brough, P. Babal, J.J. Kelly, M. Li, and T. Stevens.** Store-operated calcium entry promotes shape change in pulmonary endothelial cells expressing Trp1. *Am.J Physiol.* 275: L574-L5821998.

38. **Morais, C.J., C. Petosa, M.J. Sutcliffe, S. Raza, O. Byron, F. Poy, S.M. Marfatia, A.H. Chishti, and R.C. Liddington.** Crystal structure of a PDZ domain. *Nature* 382: 649-652, 1996.

39. **Murphy, G.M.J., X.C. Jia, A.C. Yu, Y.L. Lee, J.R. Tinklenberg, and L.F. Eng.** Reverse transcription and polymerase chain reaction technique for quantification of mRNA in primary astrocyte cultures. *J Neurosci.Res.* 35: 643-651, 1993.

40. **Nagamine, K., J. Kudoh, S. Minoshima, K. Kawasaki, S. Asakawa, F. Ito, and N. Shimizu.** Molecular cloning of a novel putative Ca2+ channel protein (TRPC7) highly expressed in brain. *Genomics* 54: 124-131, 1998.

41. **Niemeyer, B.A., E. Suzuki, K. Scott, K. Jalink, and C.S. Zuker.** The Drosophila light-activated conductance is composed of the two channels TRP and TRPL. *Cell* 85: 651-659, 1996.

42. **Okada, T., S. Shimizu, M. Wakamori, A. Maeda, T. Kurosaki, N. Takada, K. Imoto, and Y. Mori.** Molecular cloning and functional characterization of a novel receptor-activated TRP Ca2+ channel from mouse brain. *J Biol.Chem.* 273: 10279-10287, 1998.

43. **Pannetier, C., S. Delassus, S. Darche, C. Saucier, and P. Kourilsky.** Quantitative titration of nucleic acids by enzymatic amplification reactions run to saturation. *Nucleic.Acids.Res.* 21: 577-583, 1993.

44. **Petersen, C.C., M.J. Berridge, M.F. Borgese, and D.L. Bennett.** Putative capacitative calcium entry channels: expression of Drosophila trp and evidence for the existence of vertebrate homologues. *Biochem.J* 311 (Pt 1): 41-44, 1995.

45. **Philipp, S., A. Cavalie, M. Freichel, U. Wissenbach, S. Zimmer, C. Trost, A. Marquart, M. Murakami, and V. Flockerzi.** A mammalian capacitative calcium entry channel homologous to Drosophila TRP and TRPL. *EMBO J* 15: 6166-6171, 1996.

46. **Philipp, S., J. Hambrecht, L. Braslavski, G. Schroth, M. Freichel, M. Murakami, A. Cavalie, and V. Flockerzi.** A novel capacitative calcium entry channel expressed in excitable cells. *EMBO J* 17: 4274-4282, 1998.

47. **Pollock, J.A., A. Assaf, A. Peretz, C.D. Nichols, M.H. Mojet, R.C. Hardie, and B. Minke.** TRP, a protein essential for inositide-mediated Ca2+ influx is localized adjacent to the calcium stores in Drosophila photoreceptors. *J.Neurosci.* 15: 3747-3760, 1995.

48. **Preuss, K.D., J.K. Noller, E. Krause, A. Gobel, and I. Schulz.** Expression and characterization of a trpl homolog from rat. *Biochem.Biophys.Res.Commun.* 240: 167-172, 1997.

49. **Price, T., J. Aitken, and E.R. Simpson.** Relative expression of aromatase cytochrome P450 in human fetal tissues as determined by competitive

polymerase chain reaction amplification. *J Clin.Endocrinol.Metab.* 74: 879-883, 1992.

50. **Putney, J.W.J.** Type 3 inositol 1,4,5-trisphosphate receptor and capacitative calcium entry. *Cell Calcium* 21: 257-261, 1997.

51. **Putney, J.W.J.** TRP, inositol 1,4,5-trisphosphate receptors, and capacitative calcium entry [comment]. *Proc.Natl.Acad.Sci.U.S.A.* 96: 14669-14671, 1999.

52. **Sakura, H. and F.M. Ashcroft.** Identification of four trp1 gene variants murine pancreatic beta-cells. *Diabetologia* 40: 528-532, 1997.

53. **Scott, K., Y. Sun, K. Beckingham, and C.S. Zuker.** Calmodulin regulation of Drosophila light-activated channels and receptor function mediates termination of the light response in vivo. *Cell* 91: 375-383, 1997.

54. **Shieh, B.H. and M.Y. Zhu.** Regulation of the TRP Ca2+ channel by INAD in Drosophila photoreceptors. *Neuron* 16: 991-998, 1996.

55. **Sinkins, W.G., M. Estacion, and W.P. Schilling.** Functional expression of TrpC1: a human homologue of the Drosophila Trp channel. *Biochem.J* 331 (Pt 1): 331-339, 1998.

56. **Songyang, Z., A.S. Fanning, C. Fu, J. Xu, S.M. Marfatia, A.H. Chishti, A. Crompton, A.C. Chan, J.M. Anderson, and L.C. Cantley.** Recognition of

unique carboxyl-terminal motifs by distinct PDZ domains. *Science* 275: 73-77, 1997.

57. **Tomita, Y., S. Kaneko, M. Funayama, H. Kondo, M. Satoh, and A. Akaike.** Intracellular Ca2+ store-operated influx of Ca2+ through TRP-R, a rat homolog of TRP, expressed in Xenopus oocytes. *Neurosci.Lett.* 248: 195-198, 1998.

58. **Trost, C., A. Marquart, S. Zimmer, S. Philipp, A. Cavalie, and V. Flockerzi.** Ca2+-dependent interaction of the trpl cation channel and calmodulin. *FEBS Lett.* 451: 257-263, 1999.

59. **Tsiokas, L., T. Arnould, C. Zhu, E. Kim, G. Walz, and V.P. Sukhatme.** Specific association of the gene product of PKD2 with the TRPC1 channel. *Proc.Natl.Acad.Sci.U.S.A.* 96: 3934-3939, 1999.

60. **Tsunoda, S., J. Sierralta, Y. Sun, R. Bodner, E. Suzuki, A. Becker, M. Socolich, and C.S. Zuker.** A multivalent PDZ-domain protein assembles signalling complexes in a G-protein-coupled cascade. *Nature* 388: 243-249, 1997.

61. **Tsunoda, S. and C.S. Zuker.** The organization of INAD-signaling complexes by a multivalent PDZ domain protein in Drosophila photoreceptor cells ensures sensitivity and speed of signaling. *Cell Calcium* 26: 165-171, 1999.

62. **Vannier, B., X. Zhu, D. Brown, and L. Birnbaumer.** The membrane topology of human transient receptor potential 3 as inferred from glycosylation-scanning

mutagenesis and epitope immunocytochemistry. *J Biol.Chem.* 273: 8675-8679, 1998.

63. **Vannier, B., M. Peyton, G. Boulay, D. Brown, N. Qin, M. Jiang, X. Zhu, and L. Birnbaumer.** Mouse trp2, the homologue of the human trpc2 pseudogene, encodes mTrp2, a store depletion-activated capacitative Ca2+ entry channel. *Proc.Natl.Acad.Sci.U.S.A.* 96: 2060-2064, 1999.

64. **Wang, W., B. O'Connell, R. Dykeman, T. Sakai, C. Delporte, W. Swaim, X. Zhu, L. Birnbaumer, and I.S. Ambudkar.** Cloning of Trp1beta isoform from rat brain: immunodetection and localization of the endogenous Trp1 protein. *Am.J Physiol.* 276: C969-C9791999.

65. **Warnat, J., S. Philipp, S. Zimmer, V. Flockerzi, and A. Cavalie.** Phenotype of a recombinant store-operated channel: highly selective permeation of Ca2+. *J Physiol.(Lond.)* 518 (Pt 3): 631-638, 1999.

66. **Wu, X., G. Babnigg, and M.L. Villereal.** Functional significance of human trp1 and trp3 in store-operated Ca(2+) entry in HEK-293 cells [In Process Citation]. *Am.J Physiol.Cell Physiol.2000.Mar.;278.(3.):C526.-36.* 278: C526-C5362000.

67. **Xu, X.Z., H.S. Li, W.B. Guggino, and C. Montell.** Coassembly of TRP and TRPL produces a distinct store-operated conductance. *Cell* 89: 1155-1164, 1997.

68. **Yamazaki, K., T. Okada, Y. Mori, and I. Tanaka.** Genetic mapping of mouse transient receptor potential (Trrp) genes responsible for capacitative calcium

entry channels to chromosomes 3, 7, 9, and X. *Genomics* 51: 303-305, 1998.

69. **Zhu, X., P.B. Chu, M. Peyton, and L. Birnbaumer.** Molecular cloning of a widely expressed human homologue for the Drosophila trp gene. *FEBS Lett.* 373: 193-198, 1995.

70. **Zhu, X., M. Jiang, M. Peyton, G. Boulay, R. Hurst, E. Stefani, and L. Birnbaumer.** trp, a novel mammalian gene family essential for agonist-activated capacitative Ca2+ entry. *Cell* 85: 661-671, 1996.

71. **Zitt, C., A.G. Obukhov, C. Strubing, A. Zobel, F. Kalkbrenner, A. Luckhoff, and G. Schultz.** Expression of TRPC3 in Chinese hamster ovary cells results in calcium-activated cation currents not related to store depletion. *J Cell Biol.* 138: 1333-1341, 1997.

6. Appendix

Example Calculations

A. Competitive RT-PCR

This is an example of the calculations used to determine the number of fmol of Target mRNA / μg of total RNA from the x-intercept in log-log plots used in competitive RT-PCR. The data used in this example was obtained from the competitive RT-PCR of Trp3 in substantia nigra shown in Fig.3.

The x-intercept of curve ploted in log-log scale represents the point at which the ratio of Target product to MIMIC product band intensities are equal. The x-value give is in terms of fg of initial MIMIC plasmid. In this case, this value was 3.30.

Since the PCR products were labeled with Deoxiadenosine [α-^{33}P] Triphosphate the optical densities found using the phosphorimage represent the amount of AT base pairs in each product. Since the number of AT base pairs was not the same in the Target and MIMIC products, this difference was corrected for by caluclating the ratio of MIMIC AT base pairs to Target AT base pairs.

Ratio of Target to MIMIC ATs

Target product size = 525 bp

Target product AT content = 286 bp – ½ ATs in the primer set

= 286 bp – 9.5 bp

= 276.5 bp

MIMIC product size = 156 bp

MIMIC product AT content = 76 bp - ½ ATs in the primer set

= 76 bp – 9.5 bp

= 66.5 bp

Target ATs/MIMIC ATs = 66.5 bp/276.5 bp

= 0.240506

The fmol of initial MIMIC plasmid was calucated by determining the molecular weight of the MIMIC.

MIMIC plasmid size = 4106 bp

Avg. molecular weight of DNA = 660 Da/bp

Molecular weight of MIMIC = 4106 bp x 660 Da/bp

= 2709960 Da

Finally, the amount of initial total RNA added to each tube for the competitive RT-PCR experiment was 0.025 μg. Therefore the fmol of Target mRNA / μg of total RNA from the substantia nigra was calculated as follows.

10exp(x-intercept) x (MIMIC ATs/Target ATs) / ((molecular weight of MIMIC) x (total RNA/tube))

= $[(10^{3.30})$fg x 0.240506 x (1/2709960 Da)]/0.025 μg

= 0.0071 fmol/μg

This calculation was used for all competitive RT-PCR experiments.

B. Co RT-PCR

For Co-RT-PCR the ratio of optical densities of the Trp3 band to the Trp6 band in the same lane were simply multiplied by the ratio of AT content in Trp6 product to that in Trp3 product. This number was calculated to be 0.652803.